Effects of Shear and Electrical Properties on Flow Characteristics of Pharmaceutical Blends

Kalyana C. Pingali, M. Silvina Tomassone, and Fernando J. Muzzio
Dept. of Chemical and Biochemical Engineering, Rutgers University, Piscataway, NJ 08854

DOI 10.1002/aic.12047
Published online August 24, 2009 in Wiley InterScience (www.interscience.wiley.com).

This article examines the effects and interactions of shear rate, shear strain on electrical and flow properties of pharmaceutical blends. An unexpectedly strong relation between the flow and passive electrical properties of powders is observed to depend on the shear history of the powder bed. Charge density, impedance, dielectrophoresis, flow index, and dilation were measured for several pharmaceutical blends after they were subjected to a controlled shear environment. It was found that the increase in the shear strain intensified the electrical properties for blends that did not contain MgSt. The opposite effect was found in blends lubricated with MgSt. Different shear conditions resulted in different correlations between flow index and dilation. Flow properties of powders were found to improve with continuous exposure to shear strain. It was also found that flow properties correlated to charge acquisition and impedance for different shear treatments. © 2009 American Institute of Chemical Engineers *AIChE J,* 56: 570–583, 2010

Keywords: shear, electrostatics, charge density, impedance, dielectrophoresis, powder flow, composition

Introduction

Over the last few years, several approaches have been developed for improving the flow properties of pharmaceutical powders involving dry or wet granulation and addition of a flow enhancing ingredient (glidant) and magnesium stearate (MgSt). However, these empirical methods are poorly understood from a mechanistic point of view. Electrical properties of powders are often mentioned by practitioners as possible contributing factors to flow problems. Parameters such as particle size, shear stress, and consolidation time have been found to impact surface charge densities.[1,2] Particle charging is critical in many industrial processes, such as the pneumatic conveying of powders and powder blending in tumblers,[3] where it has been related to powder shear history.

However, the electrostatic and electrodynamic behavior of pharmaceutical blends remains largely an unexplored issue. Unfortunately, available technologies are only readily available for measuring monopolar charge. A more difficult problem to analyze, which is directly relevant to the formation of agglomerates and the increase of cohesion, is the acquisition of dipolar charge. This phenomenon cannot be measured using simple instruments such as by Faraday cages and electrometers and remains largely unexplored in the literature. Shear cells are one of the commonly used flow assessment methods that include compressibility studies. Both the Jenike shear cell[4] and several annular shear cells have been used to characterize the flow of pharmaceutical powders[5] under various degrees of compression. However, the range of powder densities that can be examined is somewhat limited to moderately to high degrees of consolidation, and a considerable amount of variability in results, perhaps due to environmental conditions, is quite often the observed outcome.[6]

In general, there is a need to minimize the influence of external factors during the assessment of powder flow properties. Shear history of the sample, in particular, is a factor often ignored in powder flow characterization, even though there is an awareness of its potential effects. Watano et al.[7] found that as the granules received stress in a shear mixer, a linear correlation existed between physical properties and the

Correspondence concerning this article should be addressed to F. J. Muzzio at fjmuzzio@yahoo.com

Table 1. Formulations of Pharmaceutical Blends Prepared for Measuring Flow and Electrostatic Properties

Blends	Composition (wt %)
B1	50% Avicel 102 + 50% Pharmatose
B2	9% Mic. Acetaminophen + 45.5% Avicel 102 + 45.5% Pharmatose
B3	9% Mic. Acetaminophen + 45% Avicel 102 + 45% Pharmatose + 1% MgSt
B4	9% Mic. Acetaminophen + 44.5% Avicel 102 + 44.5% Pharmatose + 1% MgSt + 1% talc
B5	9% Mic. Acetaminophen + 44.5% Avicel 102 + 44.5% Pharmatose + 1% MgSt + 1% Cab-O-Sil
B6	9% Mic. Acetaminophen + 44% Avicel 102 + 44% Pharmatose + 1% MgSt + 1% Cab-O-Sil + 1% Talc

tip speed of the shear element. An interesting study conducted by Suzuki et al.[8] revealed that strong shear forces of the impeller disrupted the long chain structures of microcrystalline cellulose. In fact, shear history, humidity, electrostatic charge acquisition, and powder cohesion are often interrelated. Particle size and relative humidity have an influence on the shear stress experienced by pharmaceutical powders.[9–11] In a study of particle separation by bipolar charge measurement system, Balachandran et al.[12] found that the electric field acts perpendicular to the flow field. In addition, bipolarly charged powders have relatively high charge-to-mass ratio.[13] In some studies, it was found that lower charge-to-mass ratio resulted in relatively high charge in individual particles.[14] A correlation between electrostatic charge level and bulk powder properties has provided basic information for the optimization of powder handling operations.[15] Therefore, the effect of charge-to-mass ratio on the electrostatic charge distribution of particles can be of technological importance in determining flow properties.

The aforementioned studies show that electrostatic charge distributions, in general, and bipolar charge specifically, can influence the transport of individual particles. The work reported here was undertaken to verify the effect of shear on electrostatics and powder flow in pharmaceutical blends. The remainder of this article is organized as follows: the Experimental section describes the experimental methods used to examine the electrical effects caused by shear environment. In the Results and Discussion section we present the results for multiple pharmaceutical blends, showing that shear rate and shear strain have a dramatic effect on electrical properties. We examine in detail the inter-relations among electrical properties of blends, and develop statistical models that account for almost all the observed variability as a function of blend composition, shear rate, strain, and their interactions. Subsequently, we demonstrate that electrical properties strongly influence, and in fact, largely predict, the powder flow properties. The last section is devoted to conclusions.

Experimental

Sample preparation

Several sets of formulations of pharmaceutical powders containing pharmatose (DMV International, Veghel, Netherlands; 100 μm), micro crystalline cellulose (avicel 102, FMC Biopolymer, Philadelphia; 90 μm), micronized acetaminophen (APAPP, Mallinckrodt, Raleigh, NC; 19 μm), magnesium stearate (Mallinckrodt, St. Louis, MO; 38 μm), talc (Barretts Minerals, Dillon, MT), and colloidal silica (Cab-O-Sil; Grade: M-5P; Cabot Corporation, Tuscola, IL 0.2 to 0.3 μm) were preblended in a v-blender and later processed at different shear conditions in a modified Couette shear cell rheometer. All blend compositions are summarized in Table 1. As a Couette cell (Figure 1) is not a good axial mixer, all the powders were premixed in a 3.8 L v-blender for 10 min to obtain a grossly homogeneous preblend of lubricant and excipients. A 50-50 mixture of pharmatose and avicel 102 was used as an excipient and mixed with 9% (on a mass basis) micronized acetaminophen (active pharmaceutical ingredient, API) in all the blends. Magnesium stearate was used as a lubricant whereas talc and colloidal silica (Cab-O-Sil) were used as antistick/flowing additives. The percentage of lubricant and additives in the blends was limited to 1% each. Therefore, the maximum concentration of lubricant and additives in the blend of excipient and API is limited to 3%.

A 3×3 factorial design is used to examine the effects of shear rates for similar amounts of strain, and the effect of strain at a constant shear rate for a wide range of treatment conditions. Every powder premixed in the v-blender was subjected to a shear rate of 5, 20, and 80 rpm and a total shear strain of 40, 160, and 640 revolutions in the shear cell rheometer. The purpose was to expose the powders to minimum, average, and maximum shear rate and strain and subsequently test for their electrical and flow properties. Uniformly spaced pins in a modified Couette cylindrical cell create a uniform shear environment. Because of the size of the controlled shear instrument, the sample size was limited to 300 g at a time. However, to measure flow index and dilation, 1815 g of powder from each blend is typically needed. Thus, a larger sample for each formulation in Table 1 was prepared by exposing multiple subsamples to a common shear treatment condition.

Experimental procedures

Experiments were performed in three stages. In the first stage, blends were prepared for a given composition, shear rate, and strain. In the second stage, three electrical properties, bulk impedance, charge density, and dielectrophoresis (adhered mass per charged surface, AMCS), were measured for each powder sample. In the third stage, characterization of flow properties of the powder blends was performed by measuring the flow index in the gravitational displacement rheometer (GDR), and dilation in a transparent horizontal rotating cylinder. Both techniques have been described in our previous work.[16,17]

Figure 2a shows the equipment used for measuring monopolar charge density. Sheared powder samples (200 g) were discharged and received in a moving train of aluminum collecting receptacles. The charge was measured at various stages of discharge. The receiving receptacle was insulated from ground and was placed using insulating tongs in an aluminum cup which was connected to a Trek electrometer. The cup was contained in a grounded Faraday cage to limit spurious charge effects. Each receptacle was weighed and charge per gram measurements was recorded. The measurement was repeated three times for each sample, and an average result was reported. The results were plotted as mass on

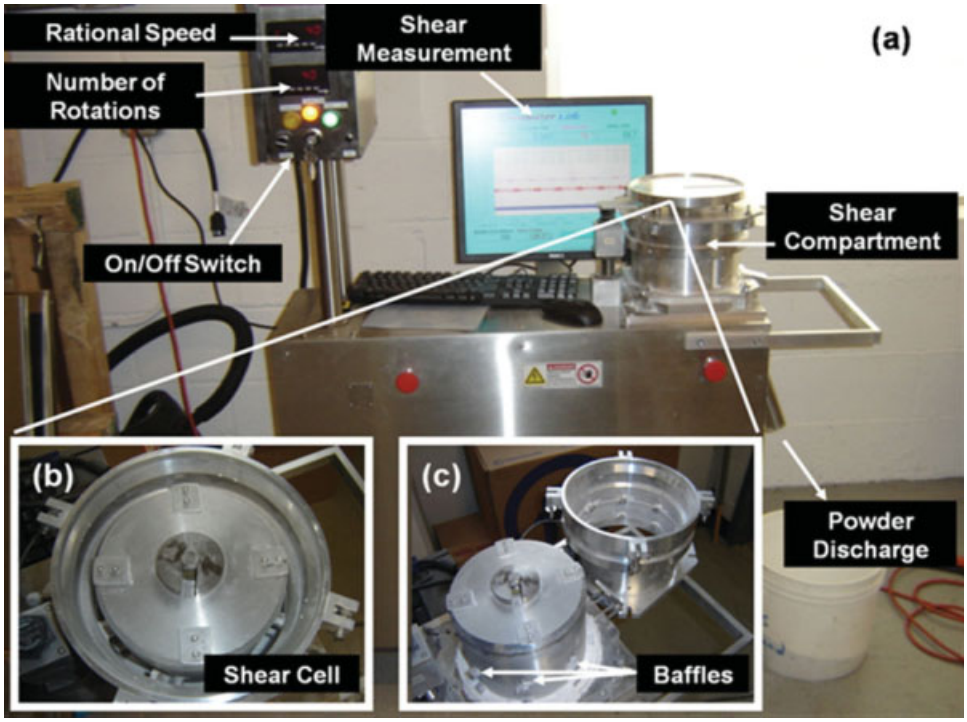

Figure 1. (a) Rutgers controlled shear environment. (b) Shear compartment where the powders processed were limited to 200 g per run due to the limited size. (c) The baffles provide the shear stress to the powder particles.

[Color figure can be viewed in the online issue, which is available at www.interscience.wiley.com.]

X-axis and charge in coulombs on *Y*-axis. The charge density was then measured from the slope of the lines as coul/g. A detailed discussion of the methodology for the measurement of charge density was presented elsewhere.[18]

Bulk impedance was measured for each of the powder blends detailed in Table 1. To measure impedance, a small powder sample (40 g) was loaded in a cylindrical cup with a conductive bottom and a nonconductive wall. The sample was then confined by applying a second electrode as a lid. A sinusoidal voltage was then applied to the top and bottom electrodes. The impedance of the powder was measured by supplying the voltage through an amplifier, using a signal generator to supply current with a given frequency to the amplifier as seen in Figure 2b. Intensities were read on an oscilloscope and impedance was then calculated over the frequency range of 10 Hz to 100 kHz. The experimental technique for measuring bulk impedance was discussed in detail in a previous publication.[16]

A van De Graaff generator (VDG), a simple electrostatic generator shown in Figure 2c, was used to measure the AMCS as a function of applied voltage. A Trek 217 electrometer was used in series with a resistor (2 GΩ) and in parallel to another grounded wire variable resistor. The intensity of current passing through the wire was controlled by moving the tip of the wire farther and nearer to the VDG. The current running through the known large resistor was monitored to calculate the voltage. A metal rod attached to a movable jog was positioned directly over VDG and was immersed 6 mm into the powder container. The VDG was activated and the rod was quickly raised after the voltage reached a steady value. Material adhered to the rod was collected and weighed. The measurement was repeated five times for each sample and an averaged result was reported. Further details about this technique can be found elsewhere.[19]

Two flow properties were measured for the powders prepared: the flow index under dynamic density conditions was measured using the GDR, and dilation was measured in a simple drum tumbler. Figure 3 shows the equipment used for measuring the flow properties. The powder is loaded on a rotating drum mounted on a hinged table that is supported by a load cell. The cylinder is filled to 40% of its volume and is rotated at 5, 10, 15, and 20 rpm to measure the flow index. As powder cohesion increases, the size of avalanches also increases, and the force signal recorded in the load cell increases correspondingly. The standard deviation of the weight signal recorded by the load cell, averaged over the range of 5 to 20 rpm, is used to define the flow index. A detailed discussion of techniques for flow measurements can be found in our previous publications.[16,17]

Results and Discussion

Effect of shear rate, strain, and blend composition on electrical properties

The effect of blend composition, shear rate, and strain on electrical and flow properties of blends was investigated using the methods described in the previous section. In the following section, we discuss the electrical properties.

Monopolar Charge Density. Charge density was measured for each of the blends and each of the shear treatments

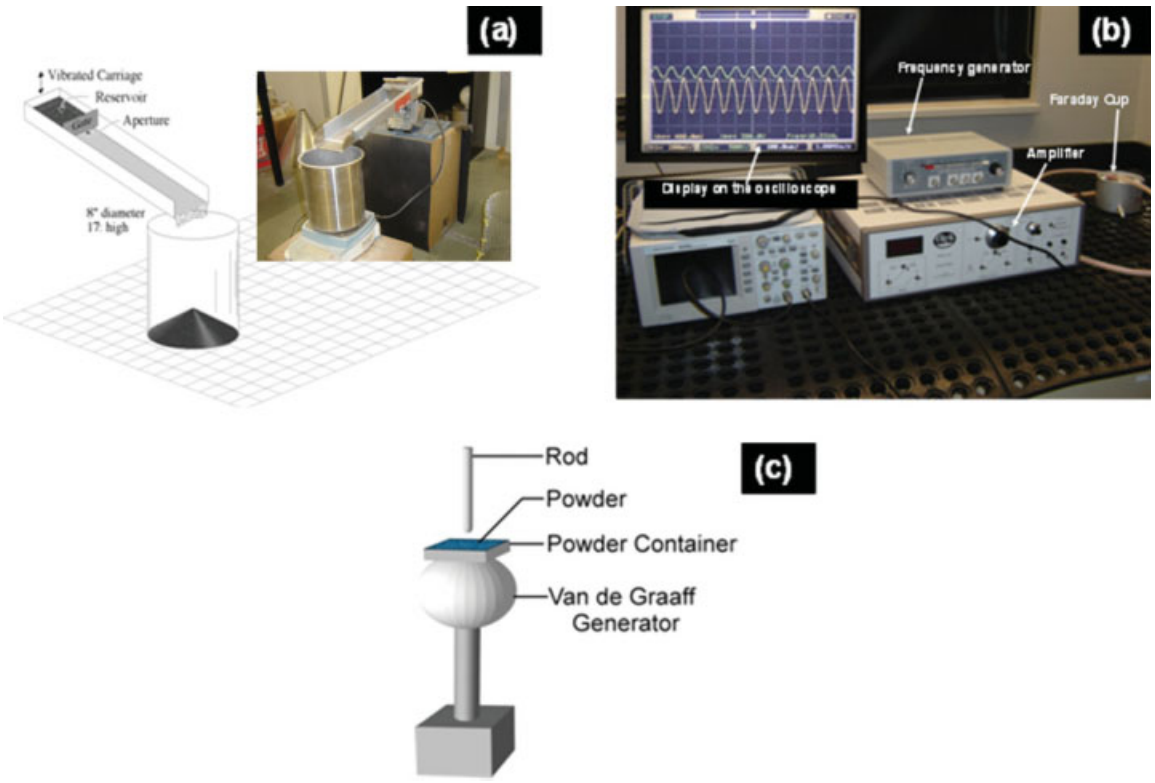

Figure 2. Experimental apparatus for measuring (a) charge density,[18] (b) impedance, and (c) electrophoresis (adhered mass per charged surface).[19]

[Color figure can be viewed in the online issue, which is available at www.interscience.wiley.com.]

listed in Table 1. It is clear from Figure 4 that blend composition plays the major role on charge acquisition. The effects of shear rate and strain, on the other hand, require further analysis. From Figure 4, it is immediately apparent that strain has a significant effect on charge accumulation, and it is also clear that the effect of strain is composition-dependent (i.e., strain and composition have a significant interaction). First, in Figure 4a, the main excipients are preblended and exposed to shear. It is evident from the figure that the charge density increased upon continuous exposure of powders to shear strain. Subsequently, Figure 4b illustrates the effect of shear on charge accumulation when API is added to the blend. An increase in the charge density is observed. For these two blends, the effect of strain is to increase total charge.

Figures 4c–f display results for four additional cases (B3–B6) where MgSt (4c), MgSt + talc (4d), MgSt + Cab-O-Sil (4e), and MgSt + talc + Cab-O-Sil (4f) are added to the excipient-API blend. Surprisingly, for all blends containing MgSt, the opposite effect of shear is observed: a decrease in

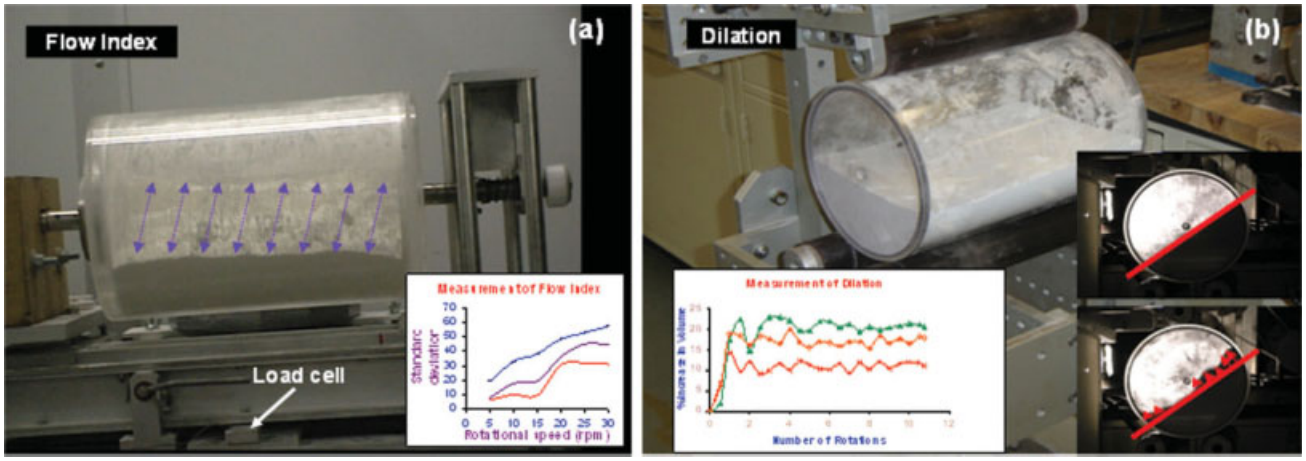

Figure 3. Equipment for measuring (a) flow index and (b) dilation (Pingali et al., submitted).

[Color figure can be viewed in the online issue, which is available at www.interscience.wiley.com.]

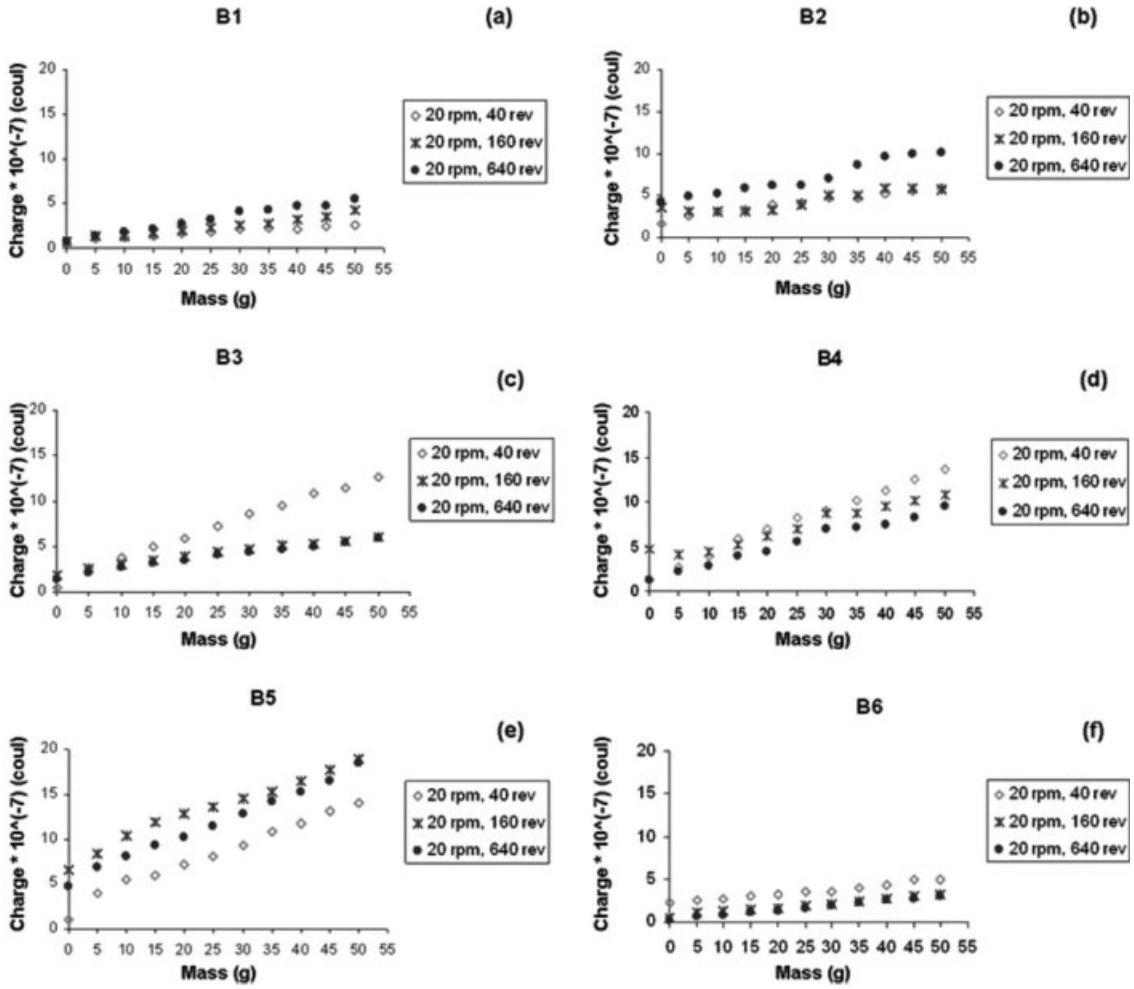

Figure 4. Variation of charge density with shear rate of 20 rpm and strain of 40, 160, and 640 rev in multiple formulations.

charge density is observed with increase in shear strain from 40 to 640 revolutions. Cab-O-Sil and talc had also substantial effects on the effects of shear on charge accumulation, although it appears that the largest effect was caused by the presence or absence of MgSt. Nonlubricated blends acquired more charge per mass as strain increases whereas lubricated blends display lower charge density at higher strain levels. This can be attributed to the nonconductive nature of MgSt. With an increase in shear forces, the disruption in the structure of particles can be expected to improve the distribution of lubricant. The interparticle interactions can possibly decrease due to the lubricant and consequently decrease the charge density. The results of charge per mass were reproducible and the observed trend was successfully repeated multiple times. To the best of our knowledge, the ability of MgSt to dramatically affect electrostatic behavior of pharmaceutical blends, and the obvious effect of strain, has not been explored in sufficient detail in the literature.

To determine not just main effects but also interactions, the data was analyzed by conducting an ANOVA using a

Table 2. Statistical Study (Analysis of Variance) of Charge Density from Different Pharmaceutical Blends (B1–B6) at Different Shear Rate and Shear Strain

Source of Variation	Sum of Squares	Degrees of Freedom	Mean of Squares	F	P-value	F-critical
Blend	0.231	5	0.046	60.154	2.30768×10^{-11}	2.711
Shear rate	0.007	2	0.003	4.318	0.028	3.493
Strain	0.002	2	0.001	1.060	0.365	3.493
Blend × shear rate	0.053	10	0.005	6.939	0.000	2.348
Blend × strain	0.018	10	0.002	2.304	0.054	2.348
Shear rate × strain	0.004	4	0.001	1.370	0.280	2.866
Error	0.015	20	0.001			
Total	0.330	53				

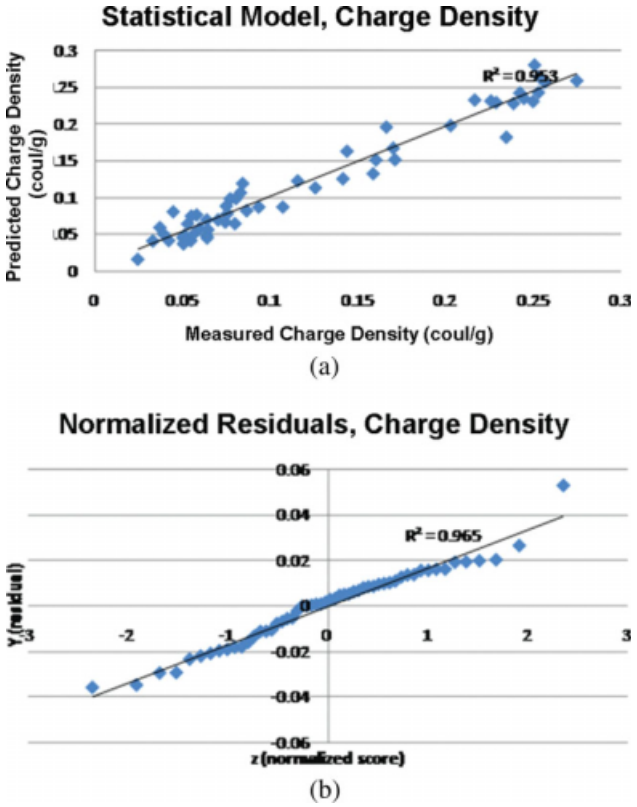

Figure 5. (a) Comparison between predicted and observed values for charge density. The factors blend, shear rate, and strain, and their two-way interactions account for 95% of all the variability in the data set. (b) Test of normality for residuals of the observed charge density measurements. Clearly, the residuals are normally distributed.

[Color figure can be viewed in the online issue, which is available at www.interscience.wiley.com.]

generalized linear model assuming, as customary, independence and normality of the data. Since only fractional replications were used to determine reproducibility, only one replication is used for the analysis. This means, in practice, that some higher order interactions need to be discarded in order to release degrees of freedom to build an error term. As a first attempt, we neglect the higher order interaction between composition, shear rate, and strain, while retaining all main effects and all two-way interactions. These assumptions determine the following model for the ANOVA:

$$Y_{ijk} = \mu + B_i + R_j + BR_{ij} + S_k + BS_{ik} + RS_{jk} + \varepsilon_{ijk} \quad (1)$$

where Y_{ijk} is the observed value for a given blend B_i, shear rate R_j, and strain S_k; BR_{ij} is the blend-shear rate interaction, BS_{ik} is the blend-strain interaction, and RS_{jk} is the shear rate-strain interaction. Finally, ε_{ijk} is the error term (or residual).

The resulting ANOVA analysis, shown in Table 2, is quite revealing. As expected, blend composition has a large, highly significant effect. Shear rate also, and not unexpectedly, has a significant effect of charge acquisition, and moreover, a clear significant interaction is observed between blend composition and shear rate. On the other hand, strain, as a main factor, is not significant by itself, but only through its interactions with blend composition (as revealed in Figure 4, which shows that for some blends, strain increases charge acquisition, while for some other blends, it decreases charge acquisition). Finally, the interaction between shear rate and strain can be neglected, as shown in the ANOVA.

As expressed in Eq. 1, the model captures 95% of the variability of the data set when all factors and two-way interactions are retained, leaving only 5% unexplained. The model also accounts for 88% of the total variability when strain and all of its interactions are discarded.

While one would normally discard the nonsignificant terms and all their interactions, in the present case, we choose to retain all the terms in Eq. 1 to compute a predicted value and a residual for each observation. The reason for this choice is that from the data, strain appears to have a large, highly nonlinear effect, rather than a negligible one. The result is displayed in Figure 5a, which shows the high degree of correlation between observed and predicted values, and in Figure 5b, which shows that the residuals defined by Eq. 1 are very close to normal, having a regression coefficient R^2 with respect to a normal distribution of 0.97.

Impedance. Subsequent measurements of conductivity of sheared samples were carried out using the same powders which had been sheared at different shear conditions in the previous section. The results of variation of electrical impedance with shear conditions of powders are shown in Table 3, and are graphically displayed in Figure 6. The trends observed for impedance measurements were similar to that of the results for charge density. Again, results indicate that the sheared lubricated blends behave differently than sheared nonlubricated blends. Tests were repeated three times for impedance measurements and results showed that as strain

Table 3. Measured Values of Impedance for Blends B1–B6 at Different Shear Rate and Shear Strain Conditions

		Impedance (ohms)					
Shear Rate (rpm)	Shear Strain (rev)	B1	B2	B3	B4	B5	B6
5	40	280.00	354.6	845.38	412.87	545.60	407.40
	160	430.76	500.00	507.61	351.56	425.88	352.76
	640	625.00	607.25	366.97	246.66	344.82	274.80
20	40	185.71	400.00	725.00	453.12	469.66	363.63
	160	358.53	609.09	472.44	376.34	347.44	326.19
	640	430.92	700.00	344.82	273.33	281.49	232.06
80	40	143.88	466.66	557.14	536.15	413.41	314.63
	160	307.69	801.96	364.46	466.14	263.92	246.30
	640	384.61	866.66	339.11	350.00	238.27	159.23

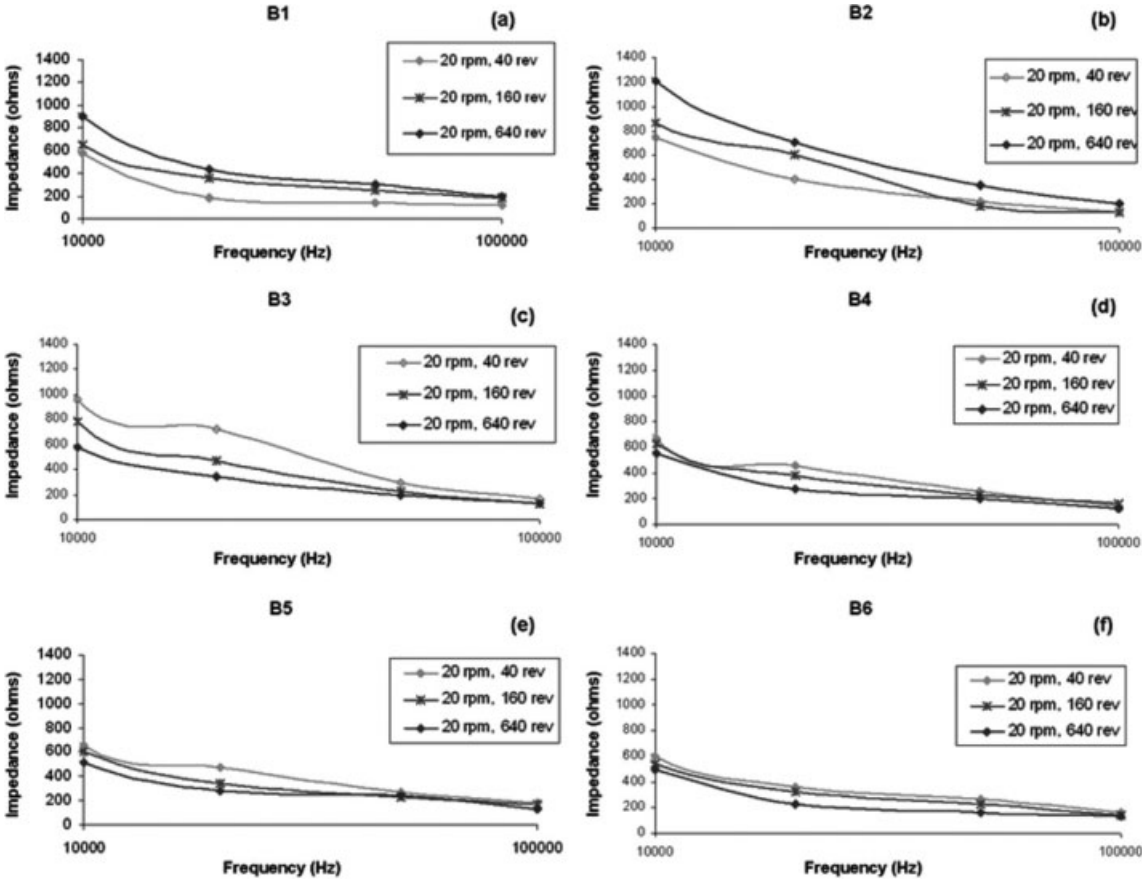

Figure 6. Effect of shear on impedance at a shear rate of 20 rpm and shear strain of 40, 160, and 640 rev.

increased, impedance always increased for nonlubricated blends and always decreased for lubricated blends, clearly pointing out to nonlinear effects of strain and significant interactions between blends and strain.

Once again, we use Eq. 1 to perform an ANOVA, which yields the results shown in Table 4. The impedance data is even cleaner than the charge acquisition data, and for this response, all three main factors are significant, as well as the interactions between blend and shear rate, and between blend and strain. On the other hand, the interaction between shear rate and strain is clearly not significant. The resulting model yields an excellent correlation between predicted and observed values (Figure 7a), explains almost 98% of the variance in the data set when all factors and two-way interactions are retained, and 97% when only the statistically significant factors are retained. The model displays nearly perfectly normal residuals, having a regression coefficient R^2 with respect to a normal distribution of 0.97 (Figure 7b).

Dielectrophoresis. The results of the dielectrophoresis measurements, which quantified the AMCS for sheared blends, are shown in Table 5 and graphically depicted in Figure 8. While results for this material response are considerably noisier than for charge density and impedance, the effects of shear rate and strain for nonlubricated blends exhibited similar trends to those observed for charge density and impedance. However, blends containing MgSt responded differently to variation in shear rate and strain. At low shear rate conditions (20 rpm) adhered mass increased as strain

Table 4. Statistical Study (Analysis of Variance) of Impedance from Different Pharmaceutical Blends (B1–B6) at Different Shear Rate and Shear Strain Conditions

Source of Variation	Sum of Squares	Degrees of Freedom	Mean of Squares	F	P-value	F-critical
Blend	532243.2	5	106448.6	72.634	3.95828×10^{-12}	2.711
Shear rate	13574.93	2	6787.466	4.631	0.022	3.493
Strain	18228.16	2	9114.082	6.218	0.007	3.463
Blend × shear rate	208431.4	10	20843.14	14.222	5.0522×10^{-7}	2.348
Blend × strain	599390.2	10	59939.02	40.899	4.08381×10^{-11}	2.348
Shear rate × strain	5610.956	4	1402.739	0.957	0.452	2.866
Error	29310.7	20	1465.535			
Total	1406790	53				

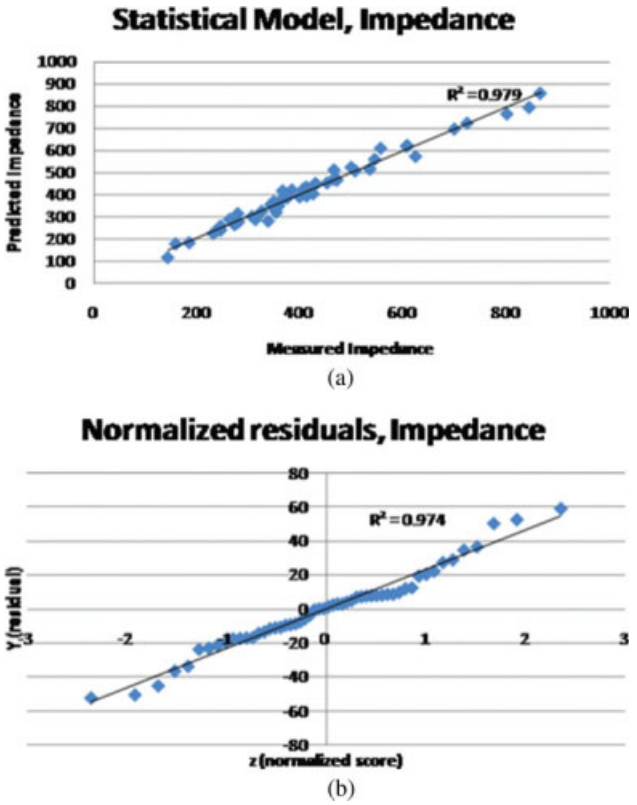

Figure 7. (a) Comparison between predicted and observed values for impedance. The factors blend, shear rate, and strain, and their two-way interactions account for 98% of all the variability in the data set. (b) Test of normality for residuals of the observed impedance measurements. The residuals are normally distributed, displaying a R^2 of 0.97 when compared to a normal distribution.

[Color figure can be viewed in the online issue, which is available at www.interscience.wiley.com.]

increased. However, the opposite trend was observed when the shear rate was increased from 20 to 80 rpm; at the higher shear rate, adhered mass decreased as strain increased. Partly, this is explained by the increased conductivity (lower impedance) of the blends that was observed for the impedance measurements; the more conductive the blend, the smaller the dielectrophoretic effect. These results are in qualitative agreement with the earlier discussions that the electrostatic accumulation in the powder bed is sensitive to the shear rate, strain and the presence of lubricant (magnesium stearate).

As in the previous two cases, we use Eq. 1 to perform an ANOVA, which is shown in Table 6. All three main factors are significant, as well as the interactions between blend and shear rate, and between shear rate and strain. For this property, however, the interaction between blend and strain is not significant. Again, excellent correlation between predicted and observed values (Figure 9a) explains 92% of the variance in the data set when all factors are retained, and 87% when only the statistically significant factors are retained. The model displays essentially normal residuals, having a regression coefficient R^2 with respect to a normal distribution of 0.97 (Figure 9b).

Regression Behavior Among Electrical Properties. This qualitative similarity in results between charge density, impedance, and dielectrophoresis suggests a correlation between these responses. Understanding the reason for similarities and differences can also help unravel the observed complex dependences on shear rate and strain, and even more importantly, to understand the basic mechanisms for the effect of lubricants and additives. To examine this issue, we first attempted a direct correlation of the results in Figure 4 and Tables 3 and 5. Regression results (not shown) were disappointing, showing a weak degree of correlation and significant scattering.

A possible reason for this is that the experimental results displayed in Figure 4 and Tables 3 and 5 were collected over a period of multiple months, where the three properties were measured using different samples, by different people, and with a highly variable degree of exposure to temperature and environmental moisture. While measurement were robust enough to allow determination of the effects of composition and shear treatment, as demonstrated in the previous three sections, the likely more tenuous correlation between properties across blend compositions and shear treatments did not survive this degree of experimental error.

To explore this issue further, a new set of blends was prepared, and for each sample, small aliquots were used to test charge acquisition, impedance, and dielectrophoresis within a short period of time. Further as discussed in later sections, flow properties were also measured for each of these samples. As explained in Section 2, testing flow properties requires a much larger amount of powder, and sample preparation becomes quite labor intensive. Thus, a smaller range of conditions was tested, where the only shear rate examined

Table 5. Measured Values of Dielectrophoresis (Adhered Mass per Charged Surface) for Blends B1–B6 at Different Shear Rate and Shear Strain Conditions

		Adhered Mass/V (g/Kv)					
Shear Rate (rpm)	Shear Strain (rev)	B1	B2	B3	B4	B5	B6
5	40	0.0119	0.0025	0.0331	0.0131	0.0025	0.005
	160	0.0038	0.0025	0.0356	0.0469	0.0044	0.0031
	640	0.0037	0.0106	0.0431	0.0469	0.0044	0.0044
20	40	0.0793	0.0054	0.0184	0.0025	0.0025	0.0044
	160	0.0804	0.0036	0.0275	0.0056	0.0025	0.0031
	640	0.0891	0.0033	0.0285	0.0094	0.0063	0.0044
80	40	0.0669	0.0588	0.055	0.0238	0.0344	0.0044
	160	0.0025	0.0031	0.035	0.0138	0.005	0.015
	640	0.0556	0.0569	0.0325	0.0469	0.0544	0.0056

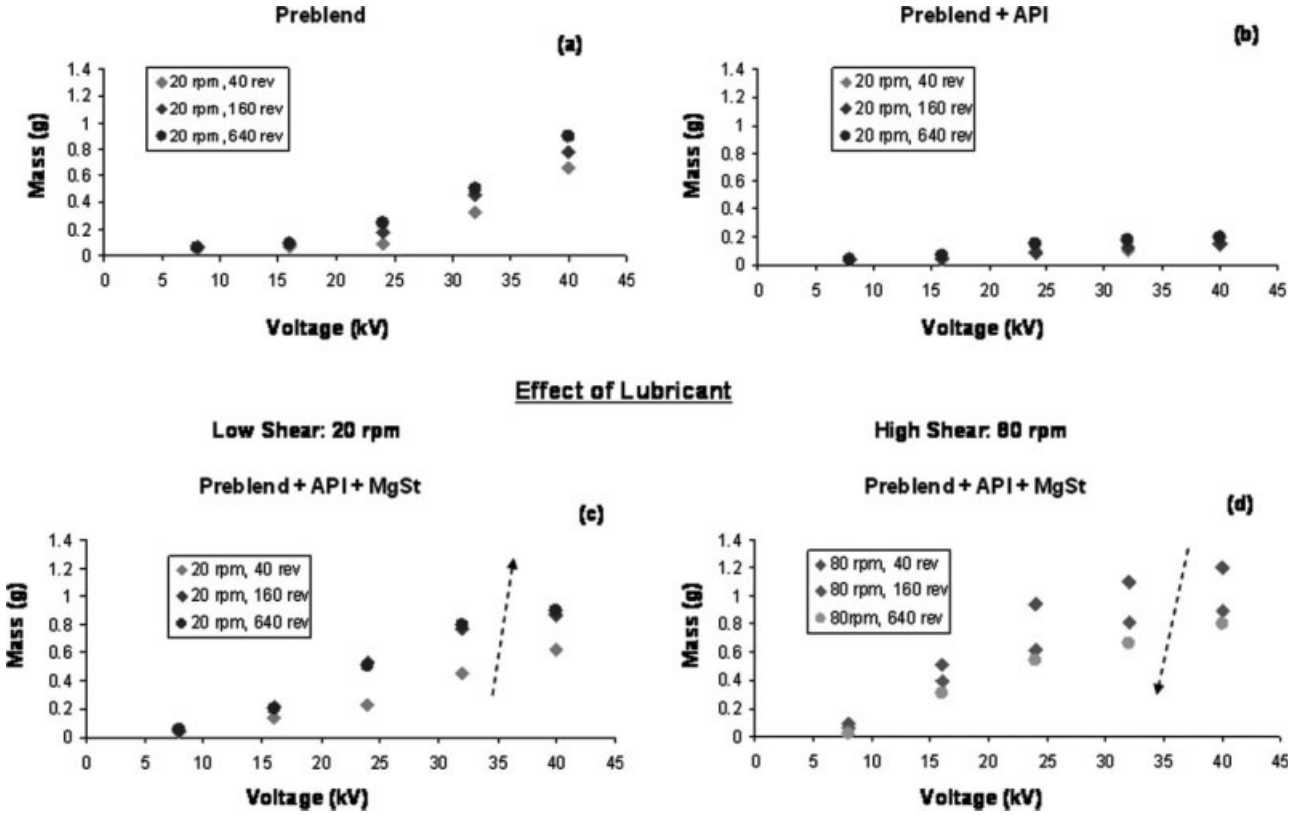

Figure 8. Dielectrophoretically adhered mass per charged surface (AMCS) as a function of shear treatment.

Unlike charge density and impedance, strain increased the adhered mass only at the low shear rate of 20 rpm. As the shear rate increased to 80 rpm, a decrease in the AMCS was observed.

was 80 rpm. Results for all five variables for each sample tested are shown in Table 7.

Results obtained with the new set of samples were extremely promising. The correlation between charge density and impedance is shown in Figure 10a. The overall data set has a regression coefficient across all formulations and strain levels of 0.68 ($F = 34.28$, $P = 2.4E\text{-}5$), and as shown in the figure, even higher regression coefficients are observed for data sets corresponding to single strain levels: for 40 revolutions, we observe $R^2 = 0.72$ ($F = 10.31$, $P = 0.0325$), for 160 revolutions, we observe $R^2 = 0.91$ ($F = 38.28$, $P = 0.003$), and for 640 revolutions, we observe $R^2 = 0.84$ ($F = 21.29$, $P = 0.01$).

The correlation between AMCS and impedance is shown in Figure 10b. Again, when tested for a single sample under similar environmental exposures, there is a high degree of correlation among measurements. The overall data set has a regression coefficient across all formulations and strain levels of 0.53 ($F = 18.46$, $P = 0.0005$), and once again, an even higher degree of correlation data sets corresponding to single strain levels: for 40 revolutions, we observe $R^2 = 0.81$ ($F = 16.53$, $P = 0.015$), for 160 revolutions, we observe $R^2 = 0.77$ ($F = 13.35$, $P = 0.02$), and for 640 revolutions, we observe $R^2 = 0.63$ ($F = 6.91$, $P = 0.06$).

First Mechanistic Interlude: Effect of Strain and Composition on Electrical Properties. The significance of the correlation among electrical measurements is manifold. One immediate conclusion is that the measurements are robust and consistent. A second observation is that not all of them are necessary, indicating that a standard measurement

Table 6. Statistical Study (Analysis of Variance) of Dielectrophoresis (Adhered Mass per Charged Surface) from Different Pharmaceutical Blends (B1–B6) at Different Shear Rate and Shear Strain

Source of Variation	Sum of Squares	Degrees of Freedom	Mean of Squares	F	P-value	F-critical
Blend	0.009	5.000	0.002	15.516	2.72462×10^{-6}	2.711
Shear rate	0.002	2.000	0.001	10.490	0.001	3.493
Strain	0.001	2.000	0.001	5.461	0.013	3.493
Blend × shear rate	0.012	10.000	0.001	10.432	6.18598×10^{-6}	2.348
Blend × strain	0.002	10.000	0.000	1.448	0.230	2.348
Shear rate × strain	0.002	4.000	0.001	4.926	0.006	2.866
Error	0.002	20.000	0.000			
Total	0.031	53.000				

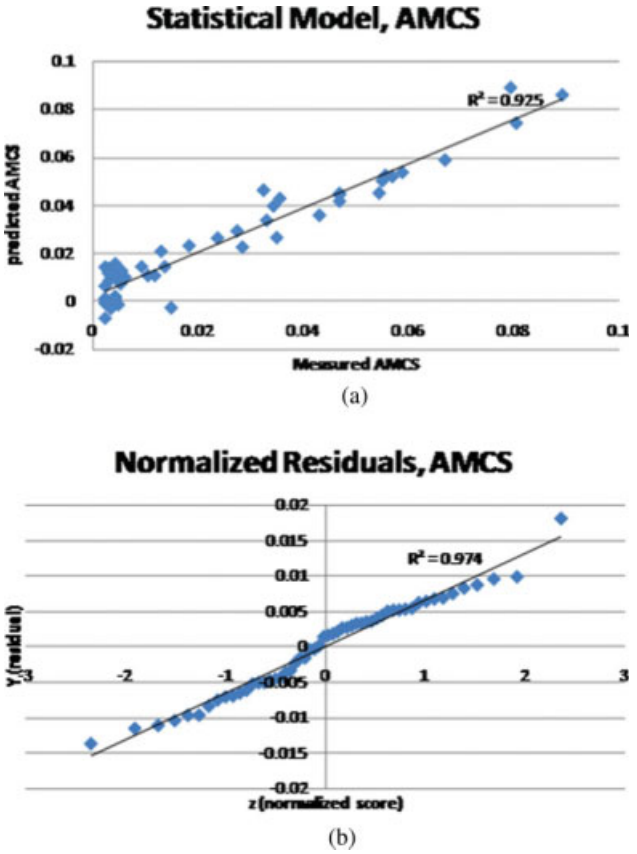

Figure 9. (a) Comparison between predicted and observed values for AMCS. The factors blend, shear rate, and strain, and their two-way interactions account for 92% of all the variability in the data set. (b) Test of normality for residuals of the observed impedance measurements. The residuals are normally distributed, displaying a R^2 of 0.97 when compared to a normal distribution.

[Color figure can be viewed in the online issue, which is available at www.interscience.wiley.com.]

might capture that important behavior, provided that the relationships among measurements are understood. A third observation is that, as previously mentioned, the relationships between measurements can be helpful in understanding the mechanisms by which shear and blend composition affect electrical behavior.

Let us start with impedance, which is the most intuitive of the three electrical measurements. Changes in impedance are directly related to the variation in the conductivity of the powder bed. This can be due to a change in composition (blend effect), a change in density, or a change in microstructure. The latter can be shear rate and/or strain dependent, for example, if an "ordered mixing" process takes place during shearing.[20,21] In such a situation, a minor ingredient with small particle size is deposited by mechanical action on the outer surface of larger, more conductive particles. If the electric conductivity of the minor and major components differs significantly, then conductivity, and hence, impedance, would depend on the chemical nature of the major and minor components (i.e., blend-dependent effects) and the degree of coating (shear and strain-dependent changes). The rate of progress of the coating process, and its eventual degree of completion, could also depend on the relative amounts of minor and major components present in the blend; thus setting the stage for the blend-shear-strain interactions observed in previous sections.

Conductivity also explains the correlation between impedance, charge density, and dielectrophoresis. As conductivity increases (and, consequently, impedance decreases), blends should release electrostatic charge more easily. Thus, the direct correlation observed between charge and impedance (Figure 10a). Similarly, more conductive blends sustain less induced dipolar charge; in fact, particles covered with conductive nanoparticles exhibit no dielectrophoresis whatsoever (LaMarche et al., submitted). Thus, as conductivity increases and impedance decreases, AMCS should decrease (as observed).

However, it is important to mention here that, as discussed later in this article, impedance can be also affected by blend cohesion: a less cohesive blend packs more densely, increasing the number of interparticle contacts and hence, the blend

Table 7. Values of Charge, Impedance, AMCS, Flow Index, and Dilation Measured for Single Samples

Blend	Shear Rate (rpm)	Shear Strain (rev)	Charge Den (coul/g)	Impedance (ohms)	Ad. Mass (g/Kv)	Flow Index	Dilation (%)
B1	80	40	0.124	270.38	0.0669	40.490	40.318
B1	80	160	0.139	218.06	0.015	30.399	30.525
B1	80	640	0.182	255.31	0.0556	22.159	28.385
B2	80	40	0.107	244.98	0.0588	35.490	39.165
B2	80	160	0.098	162.74	0.005	21.578	27.548
B2	80	640	0.215	392.15	0.0569	27.095	32.63
B3	80	40	0.093	230.76	0.055	32.720	37.187
B3	80	160	0.170	221.96	0.0138	31.931	34.166
B3	80	640	0.080	157.89	0.0325	19.363	21.202
B4	80	40	0.066	222.20	0.0238	29.610	29.004
B4	80	160	0.174	253.52	0.035	33.345	35.137
B4	80	640	0.159	295.00	0.0469	21.652	25.211
B5	80	40	0.080	188.23	0.0344	30.950	31.778
B5	80	160	0.075	173.21	0.0031	20.152	25.019
B5	80	640	0.162	217.53	0.0544	23.400	26.392
B6	80	40	0.064	160.71	0.0044	25.030	26.237
B6	80	160	0.051	122.61	0.0025	16.767	19.427
B6	80	640	0.033	108.52	0.0056	16.444	19.579

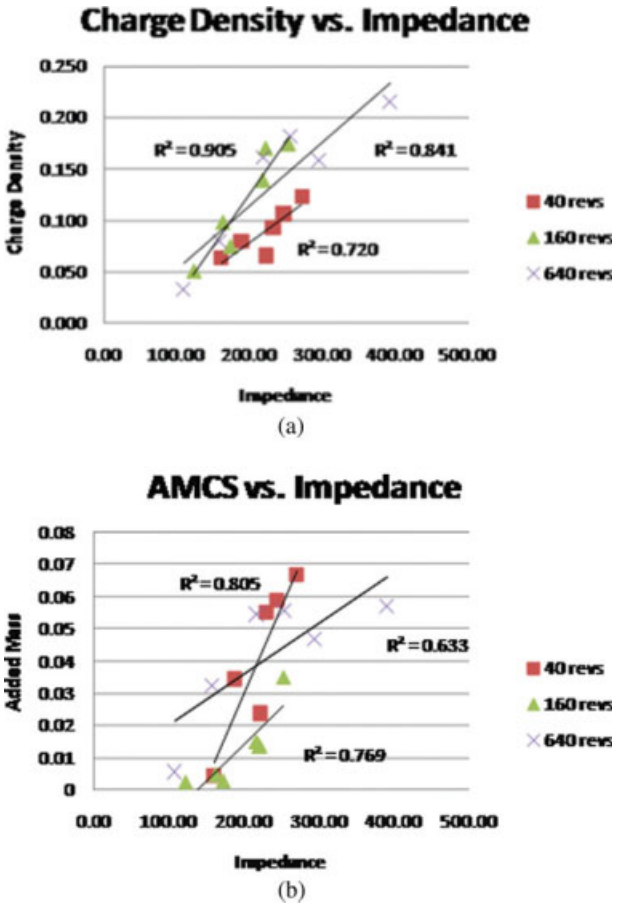

Figure 10. (a) Correlation of charge density vs. impedance for the samples in Table 6. A high degree of correlation between charge density and impedance is observed across blends and strain levels. (b) Correlation of AMCS vs. impedance for the samples in Table 7. A high degree of correlation between dielectrophoresis and impedance is observed across blends and strain levels.

[Color figure can be viewed in the online issue, which is available at www.interscience.wiley.com.]

conductivity. Blend cohesion has been shown to depend strongly on blend composition, shear rate, and strain, and it would be immediately affected by ordered mixing situations. Importantly, the ''conductivity by ordered mixing'' mechanism and the ''cohesion'' mechanism are not mutually exclusive, quite the opposite, they can both be present, and can reinforce or counteract each other. Thus, the need to examine also flow properties (discussed in the next section).

Effect of strain and blend composition on powder flow properties

Measurements of flow index and dilation, shown in Table 7, were used to examine the effect of blend composition and strain on blend cohesion. Figure 11 shows that, as in previous publications, flow index and dilation were linearly proportional to each other. The overall data set has a regression coefficient across all formulations and strain levels of 0.90 ($F = 160$, $P = 9.6\text{E-}10$). A similar degree of correlation was observed for data sets corresponding to single strain levels: for 40 revolutions, we observe $R^2 = 0.87$, for 160 revolutions, we observe $R^2 = 0.93$, and for 640 revolutions, we observe $R^2 = 0.92$.

The following three observations can be drawn from the experimental investigation of flow properties of sheared powders. First, flow properties of powder blends were sensitive to strain. As strain increased, values of flow index and cohesion for all blends shifted to the lower left corner of Figure 11, indicating a decrease in cohesion and an increase in dynamic density (tighter powder packing) as strain increased. Second, the blend composition interacts with strain, hence the change in slope of the lines in Figure 11.

Third, the trends in Table 7 and Figure 11 qualitatively agree with the electrical measurements, suggesting a possible correlation between electrostatic behavior caused by shear and powder flow.

Figures 12–14 examine the correlation between flow properties with electrical measurements. It is evident from Figure 12a that the flow index was linearly proportional to the charge density, and that the effect was strongly dependent on strain, for all blends examined here. While the entire data set correlated poorly ($R^2 = 0.1$), sets of samples for all six blends, each set corresponding to fixed levels of strain, showed a high level of correlation. For 40 revolutions, we observe $R^2 = 0.93$ ($F = 51.3$, $P = 0.002$), for 160 revolutions, we observe $R^2 = 0.97$ ($F = 150.9$, $P = 0.0002$), and for 640 revolutions, we observe $R^2 = 0.89$ ($F = 32.4$, $P = 0.005$).

Essentially identical behavior is observed in Figure 12b for dilation. While the entire data set showed poor correlation ($R^2 = 0.19$, $P = 0.07$), three distinctive, highly correlated sets were observed for the three strain levels. For 40 revolutions, we observe $R^2 = 0.92$ ($F = 46.7$, $P = 0.002$), for 160 revolutions, we observe $R^2 = 0.97$ ($F = 114.9$, $P = 0.0004$), and for 640 revolutions, we observe $R^2 = 0.92$ ($F = 49.1$, $P = 0.002$). Also interestingly, for both flow index and dilation, the six blends preserved precisely the rank order within a strain level.

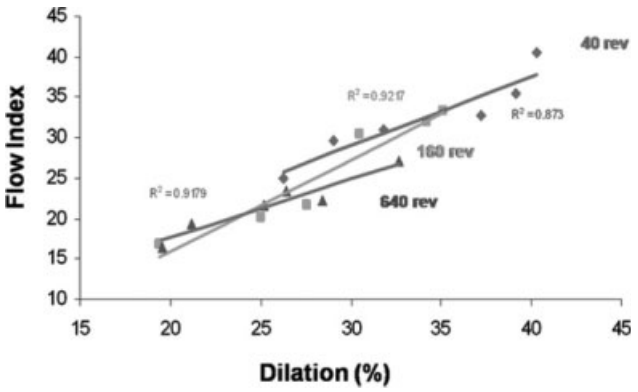

Figure 11. Flow index and dilation correlated to each other for different shear treatment.

Different shear conditions resulted in different families of correlations. Flow index decreased with an increase in the shear strain indicating a decrease in cohesion with continuous exposure to shear strain.

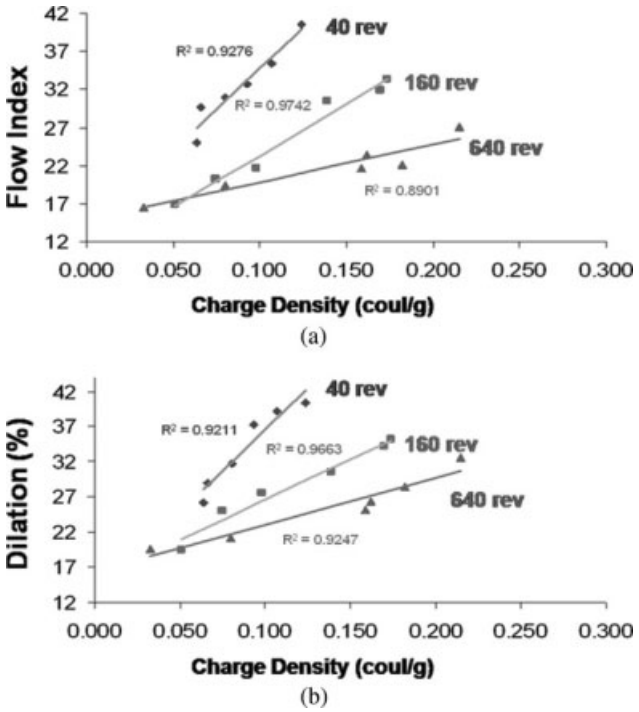

Figure 12. (a) Flow index and (b) dilation correlate to charge acquisition for different shear treatments.

Flow index and dilation increased with charge acquisition indicating worsening of powder flow with charge accumulation.

While it would be premature to conclude (as sometimes practitioners do) that electrostatic charge determines powder flow, it is clear from the results in Figures 12a, b that electrostatic charge density in fact predicts a great deal of the observed flow variability as a function of composition or strain. As a minimum, for the experiments described here, charge density correlates with flow properties, and strongly indicates the existence of a common cause for charge accumulation and changes in flow properties as a function of composition and shear.

As before, impedance is a likely candidate for a common cause for the dependence of flow properties and electric charge accumulation as a function of strain. In a previous publication, we established a strong correlation between impedance and powder flow.[16] As shown in Figures 13a, b, as impedance decreases, so do flow index and dilation. However, once again, the correlation is also dependent on shear strain. As strain increases, the slopes of the correlations of both flow index and dilation with impedance also decrease. In other words: for a fixed value of impedance, the larger the strain, the better is the flow.

Finally, Figures 14a, b also show that, for a given strain level, flow index and dilation correlate to dielectrophoretically adhered mass. Again, while the entire data set correlates poorly, for different strain levels, three highly correlated sets of results can be distinguished. However, for this property, the effect of strain on the correlation between flow properties and AMCS is nonmonotonic. For a fixed added mass level, both flow index and dilation first increase, and then decrease, as strain increases; and moreover, the correlation between flow properties and AMCS exhibits a significant degree of nonlinearity for the intermediate strain level (160 revolutions).

Second Mechanistic Interlude: Effect of Composition and Strain on Flow Properties and Electric Connection. The picture that emerges for the preceding discussion is that electrical properties and flow properties of blend are clearly inter-related, and are affected similarly by composition and strain. The question, of course, is why. As discussed earlier, and as we introduced in a previous publication, we hypothesize that generation of an ordered mixing microstructure could lead to significant changes in overall conductivity and also to substantial changes in blend cohesion. In general, the greater the strain or the more intense the shear rate, the larger the extent of the development of an ordered mixture, providing a simple explanation for the observed main effects of shear rate and strain. However, it is important to notice that multiple outcomes are possible. A decrease in interparticle forces, perhaps caused by ordered mixing, will always lead to greater density and more interparticle contacts, and would tend to increase conductivity. However, if the minor component coating the larger particles is less conductive than the main ingredients, the ordered mixture could be less conductive than the original blend. Finally, in the absence of a friable minor component, an ordered mixture would not be created. Under such conditions, strain can lead simply to the evolution of tribocharging, increasing the blend cohesion, decreasing density, and making the entire blend less conductive (as observed here for unlubricated bends).

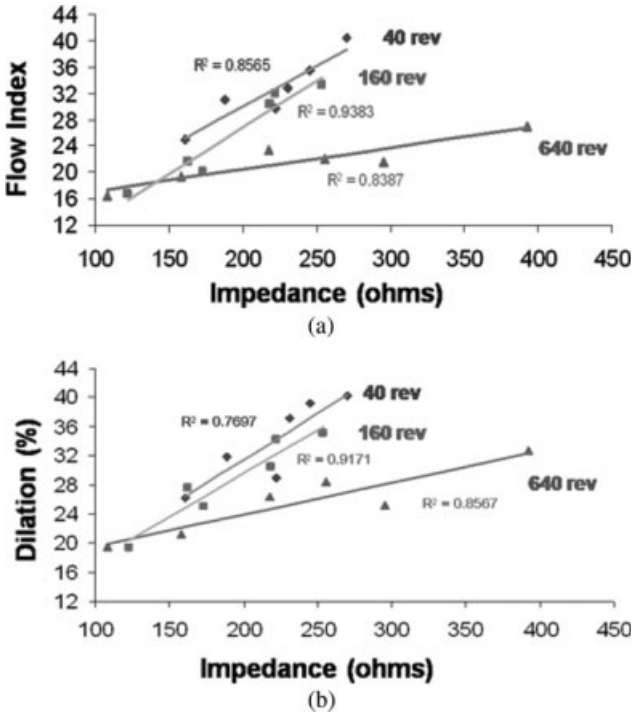

Figure 13. (a) Flow index and (b) dilation correlate to impedance for different strain treatments.

A decrease in cohesion is observed with an increase in strain.

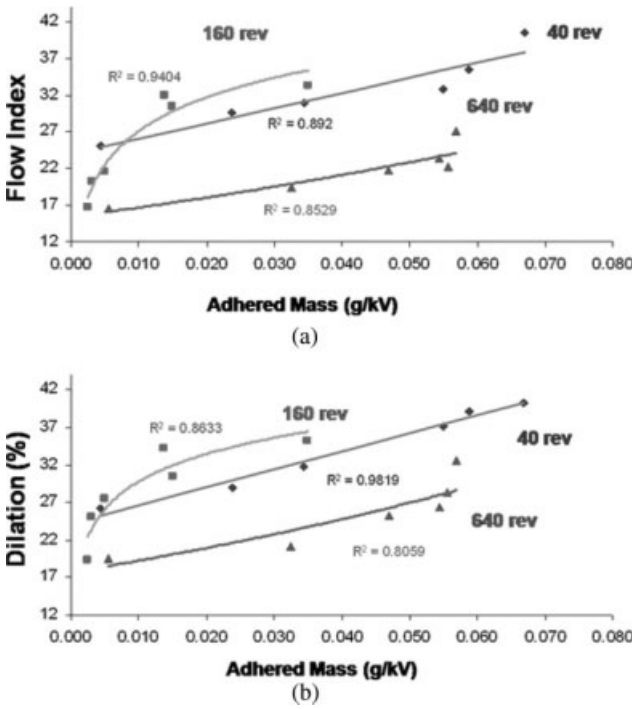

Figure 14. (a) Flow index and (b) dilation correlate to dielectrophoresis for different strain treatments.

Powder flow worsened with an increase in AMCS. The effect of strain is nonmonotonic and possibly nonlinear for the intermediate strain level.

Conclusions

This article expands significantly our previous studies where we established that flow index and dilation are linearly proportional to each other, and where we demonstrated the existence of a correlation between impedance and flow properties. Using two data sets and a factorial design involving six blend compositions and three strain levels, and three shear rate levels, several major observations were established:

- A statistical model considering main effects and two-way interactions between blend composition, strain, and shear rate explained almost all the variability observed for charge density, impedance, and electrophoretically adhered mass.
- Electrical properties of powders are strongly interrelated when measured for the same sample within a short time period.
- Effect of strain on electrical properties was strongly affected by the presence of MgSt. Charge density and impedance increased with strain for nonlubricated blends, but decreased for lubricated blends.
- Flow index and dilation exhibited a very strong correlation across blend composition and strain levels. Flow index and dilation generally decreased with strain.
- Powder flow properties correlated strongly to electric powder properties across multiple blend compositions. However, these correlations were strongly dependent on strain.

The above results and discussion demonstrate that for blends of very commonly used pharmaceutical materials, composition and shear history interact strongly to create a multivariate inter-related set of electrical and flow properties. Different families of powders prepared using different amounts of strain exhibit widely different flow and electrical properties. This is sobering, because powder flow properties are often characterized using fresh materials, or process samples developed at the pilot scale. However, the amount of strain experienced by a powder during processing is affected by the scale of the process. This means that all the effects discussed in this article are scale dependent as well.

A second observation worth mentioned to conclude this section is that while shear strain and shear rate both had an influence on electrical and flow properties of powders, the effect of shear strain was found to be much more intense than that of shear rate. This is somewhat counter intuitive; most common practices focus on the speed of mixers and feed frames, than on the total energy imparted to the blend. Such practices need to be re-examined, since it appears that strain is at least as important, and possibly more important, than shear rate, in affecting mechanical and electrical properties of blends.

Important questions remain. Why, exactly, do flow properties correlate to electrical properties, mainly impedance? Why does strain, and to a lesser extent shear rate, affect electrical properties as well as flow behavior? The hypothesis of the creation of ordered mixtures, and the interaction between changes in conductivity and packing, provide an attractive explanation that must be confirmed experimentally. Answering these questions in definite manner is essential to meaningful further progress in understanding critical in-process material properties of pharmaceutical blends.

Acknowledgments

This work was supported by the Engineering Research Center on Structured Organic Particulate Systems and by Pfizer Inc. The authors thank Michael Levin from Metropolitan Computing Corporation for material assistance and helpful discussions.

Literature Cited

1. Engers DA, Fricke MN, Storey RP, Newman AW, Morris KR. Triboelectrification of pharmaceutically relevant powders during low-shear tumble blending. *J Electrostat*. 2006;64:826–835.
2. Ramchandruni H, Hoag SW. Design and validation of an annular shear cell for pharmaceutical powder testing. *J Pharm Sci*. 2001;90:531–540.
3. Watanabe H, Samimi A, Ding YL, Ghadiri M, Matsuyama T, Pitt KG. Measurement of charge transfer due to single particle impact. *Particle Particle Syst Characterization*. 2006;23:133–137.
4. Michrafy A, Ringenbacher D, Tchoreloff P. Modelling the compaction behaviour of powders: application to pharmaceutical powders. *Powder Technol*. 2002;127:257–266.
5. Nyqvist H, Brodin A. Precision of a ring shear cell in determining flow properties of pharmaceutical powders. *Acta Pharmaceutica Suecica*. 1980;17:215–223.
6. Soh JKP, Liew CV, Heng PWS. New indices to characterize powder flow based on their avalanching behavior. *Pharm Dev Technol*. 2006;11:93–102.
7. Watano S, Okamoto T, Sato Y, Osako Y. Scale-up of high shear granulation based on the internal stress measurement. *Chem Pharm Bull*. 2005;53:351–354.
8. Suzuki T, Kikuchi H, Yamamura S, Terada K, Yamamoto K. The change in characteristics of microcrystalline cellulose during wet

granulation using a high-shear mixer. *J Pharm Pharmacol*. 2001;53:609–616.
9. Oyebola MT, Podczeck F, Barrett D. The influence of particle size and relative humidity of air on the shear properties of pharmaceutical powders. *Eur J Pharm Sci*. 2004;23:S46.
10. Rowley G. Quantifying electrostatic interactions in pharmaceutical solid systems. *Int J Pharm*. 2001;227:47–55.
11. Watanabe H, Ghadiri M, Matsuyama T, Ding YL, Pitt KG, Maruyama H, Matsusaka S, Masuda H. Triboelectrification of pharmaceutical powders by particle impact. *Int J Pharm*. 2007;334: 149–155.
12. Balachandran W, Kulon J, Koolpiruck D, Dawson M, Burnel P. Bipolar charge measurement of pharmaceutical powders. *Powder Technol*. 2003;135:156–163.
13. Yurteri CU, Mazumder MK, Grable N, Ahuja G, Trigwell S, Biris AS, Sharma R, Sims RA. Electrostatic effects on dispersion, transport, and deposition of fine pharmaceutical powders: development of an experimental method for quantitative analysis. *Particulate Sci Technol*. 2002;20:59–79.
14. Saini D, Biris AS, Srirama PK, Mazumder MK. Particle size and charge distribution analysis of pharmaceutical aerosols generated by inhalers. *Pharm Dev Technol*. 2007;12:35–41.
15. Nishiyama T, Yunoki K, Honda T, Yazawa H. Evaluation of the electrostatic properties of pharmaceutical powders during pneumatic conveying. *Nippon Kagaku Kaishi*. 1998;201–206.
16. Pingali KC, Shinbrot T, Hammond SV, Muzzio FJ. An observed correlation between flow and electrical properties of pharmaceutical blends. *Powder Technol*. 2009;192:157–165.
17. Faqih A, Chaudhuri B, Alexander AWA, Hammond S, Muzzio FJ, Tomassone MS. Dilation effects of cohesive granular material in a rotating drum: experiments and simulations. *AIChE J*. 2006;52:4124–4132.
18. Mehrotra A, Muzzio FJ, Shinbrot T. Spontaneous separation of charged grains. *Phys Rev Lett*. 2007;99:058001.
19. Shinbrot T, LaMarche K, Glasser BJ. Triboelectrification and razorbacks: geophysical patterns produced in dry grains. *Phys Rev Lett*. 2006;96:178002.
20. Hersey JA. Ordered mixing: a new concept in powder mixing practice. *Powder Technol*. 1975;11:41–44.
21. Crooks MJ, Ho R. Ordered mixing in direct compression of tablets. *Powder Technol*. 1976;14:161–167.

Manuscript received Feb. 19, 2009, revision received May 31, 2009, and final revision received July 16, 2009.